

Structure of the Fission Transition Nucleus $U^{235}\dagger$

A. N. BEHKAMI*

Northwestern University, Evanston, Illinois 60201

and

Argonne National Laboratory, Argonne, Illinois 60439

AND

J. H. ROBERTS

Northwestern University, Evanston, Illinois 60201

AND

W. LOVELAND‡ AND J. R. HUIZENGA*

Argonne National Laboratory, Argonne, Illinois 60439

(Received 1 February 1968)

Fission-fragment angular distributions for the $U^{234}(n,f)$ reaction were measured for incident neutron energies of 200, 300, 400, 500, 600, 700, 843, 998, and 1184 keV. A novel 2π geometry Lexan (polycarbonate) detector was used to detect the fission fragments. The angular distributions show intermediate-angle peaks and change shape rapidly with changes in neutron energy. Based on a sophisticated Hauser-Feshbach analysis, which includes level-width fluctuation corrections of the energy variation of the fission cross section and angular distributions, a description of the highly deformed fission transition nucleus U^{235} is given. Assignments of the quantum numbers (K,π) are made for three low-energy single-particle states, and they are $\frac{3}{2}+$, $\frac{3}{2}+$, and $\frac{3}{2}-$. In addition, the presence of another $K=\frac{3}{2}$ state is demonstrated. Assignments of the energy E and the barrier curvature $\hbar\omega$ of these states are also given.

I. INTRODUCTION

ONE of the most useful concepts in discussing nuclear fission phenomena is that of the transition nucleus. This concept,¹ first advanced by A. Bohr in 1955, suggests that as the nucleus deforms during the fission process, it reaches a state, the transition state, where most of the energy of the nucleus is tied up as deformation energy and thus the nucleus is relatively "cold," i.e., it possesses little internal excitation energy. The spectrum of quantum states in the nucleus at this point is expected to resemble the spectrum of low-lying excited states of the slightly deformed initial nucleus. Each one of these excited states can be described in terms of the quantum numbers, J , K , M , π , where J represents the total angular momentum, π is the parity of the state, K is the projection of J on the nuclear-symmetry axis, and M is the projection of J on some space-fixed axis (usually the beam axis for particle-induced fission).

The angular distribution of the fission fragments is related to these quantum numbers and for the neutron-induced fission of even-even nuclei is given by,

$$W_{MK}^J(\theta) = \frac{1}{4}(2J+1) \left[|d_{M=1/2,K}^J(\theta)|^2 + |d_{M=-1/2,K}^J(\theta)|^2 \right], \quad (1)$$

† Research performed in part under the auspices of the U. S. Atomic Energy Commission.

* Present address: Nuclear Structure Research Laboratory, University of Rochester, Rochester, N. Y.

‡ Present address: The Radiation Center, Oregon State University, Corvallis, Ore.

¹ For a general review of the transition-state concept, see J. R. Huizenga, in *Nuclear Structure and Electromagnetic Interactions*, edited by N. MacDonald (Plenum Press, Inc., New York, 1965), p. 319.

where $W_{MK}^J(\theta)$ is the angular distribution of fission fragments from the nucleus in a transition state (J,K,M) and the $d_{MK}^J(\theta)$ functions are given by

$$d_{MK}^J(\theta) = ((J+M)!(J-M)!(J+K)!(J-K)!)^{1/2} \times \sum_{X=0} \frac{(-1)^X (\sin \frac{1}{2}\theta)^{K-M+2X} (\cos \frac{1}{2}\theta)^{2J-K+M-2X}}{(J-K-X)!(J+M-X)!(X+K-M)!X!}, \quad (2)$$

where the sum is over $X=0, 1, 2, 3, \dots$ and contains all terms in which no negative value appears in the denominator for any one of the quantities in parentheses. Some typical $W_{MK}^J(\theta)$ functions are plotted in Fig. 1 and serve to illustrate the point that the "signatures" of many of the transition states are intermediate-angle peaks in the fragment angular distributions. It may be possible, therefore, to deduce the quantum numbers of these states of the transition nucleus ("the transition-state spectrum") from an analysis of the fragment angular distributions and fission cross sections in the (n,f) reaction. From an examination of Fig. 1, one can also see that the anisotropies $(\sigma(0^\circ)/\sigma(90^\circ))$ are not as sensitive as the full angular distributions to the quantum numbers of a given state.

Low-energy neutron-induced fission of even-even nuclei with fission thresholds exceeding the neutron binding energy and fairly high fission cross sections, like U^{234} , offers one of the best opportunities for characterizing the transition-state spectrum, since only a few states in the transition nucleus will be accessible and the properties of the levels in the target nucleus populated by neutron emission are known. The angular

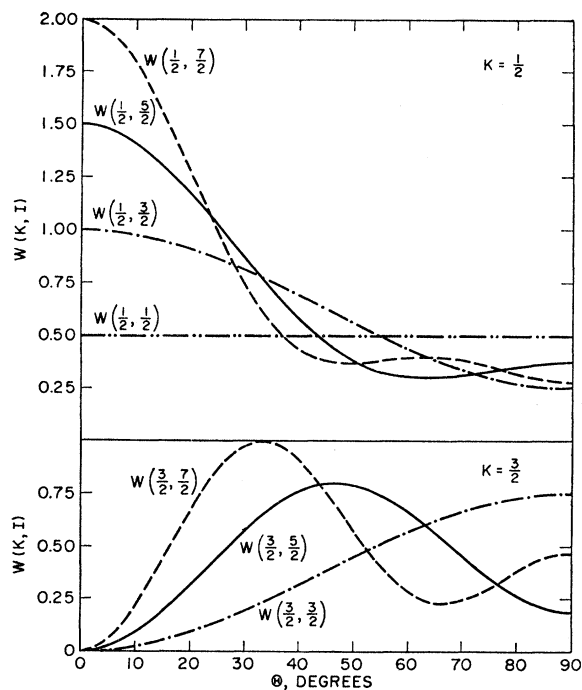


FIG. 1. Theoretical fission-fragment angular distributions for neutron-induced fission of even-even target nuclei. The axis of quantization is along the beam direction and M has values of $\pm \frac{1}{2}$. The top part of the figure is for fission through states in a band with $K = \frac{1}{2}$ and J values of $\frac{1}{2}$, $\frac{3}{2}$, $\frac{5}{2}$, and $\frac{7}{2}$. The bottom part of the figure is for fission through states in a band with $K = \frac{3}{2}$ and J values of $\frac{3}{2}$, $\frac{5}{2}$, and $\frac{7}{2}$. Each curve is normalized such that $\int_{-1}^{+1} W_{K^J}(\theta) d(\cos\theta) = 1$.

momentum of the compound nucleus will be small and restricted in direction such that $M = \pm \frac{1}{2}$.

In this paper we wish to report the results of measurements of the fission-fragment angular distributions at several energies in the $U^{234}(n, f)$ reaction. We have attempted to deduce the K quantum number, parity, energy, and barrier curvature of the states of the U^{235*} transition nucleus near the fission barrier by examining the energy variation of the angular distribution and cross section for the $U^{234}(n, f)$ reaction.² The method of deduction involves sophisticated curve fitting using a

type of Hauser-Feshbach calculation of the partial fission cross sections.

In Sec. II we describe the experimental procedures used to measure these angular distributions, and in Sec. III we present our experimental results. A discussion of theoretical methods used to analyze the data and a discussion of the results of this analysis will be found in Secs. IV and V, respectively. A critical evaluation of this method of doing transition-state spectroscopy is given in Sec. VI and the relation of our results to other data, calculations, etc. is given in Sec. VII. Section VIII gives a summary of the work.

II. EXPERIMENTAL PROCEDURES

Because of the low fission cross sections near threshold, a highly efficient method of measuring fission-fragment angular distributions had to be developed. The main feature of our experimental procedures was the use of a solid-state nuclear track detector to measure the fission-fragment angular distributions. It is well known³ that the radiation damage sites caused by fission fragments entering a number of insulating materials can be enlarged by chemical etching until they can be seen with an optical microscope. By choosing a suitable material, the number of fission events can be recorded uniquely within a high background of low-mass particles.

Before arriving at the detection scheme adopted in this experiment, two detector arrangements were investigated. The method used in this experiment is illustrated in Fig. 2, and the other method, which was not used, is described in the Appendix. Monoenergetic neutrons, produced by the $Li^7(p, n)Be^7$ reaction, impinging on an isotopically pure U^{234} target of 0.5 mg/cm² thickness. The target was tilted at an angle of 33° to avoid absorption of the fragments in the target. The neutron energy spread due to (a) the Li target thickness, (b) the U^{234} target thickness, and (c) the range of neutron angles (and, therefore, energies) subtended by the U^{234} target was 15 keV. The fission fragments from the $U^{234}(n, f)$ reaction were detected with a polycarbonate resin detector.

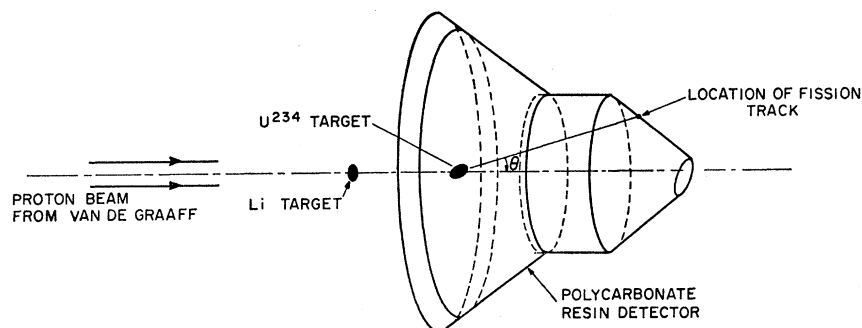


FIG. 2. Schematic diagram of the experimental apparatus.

² A preliminary account of this work was reported by W. Loveland, J. R. Huizenga, A. Behkami, and J. H. Roberts, Phys. Letters 24B, 666 (1967).

³ R. L. Fleischer, P. B. Price, R. M. Walker, and E. L. Hubbard, Phys. Rev. 133, A1443 (1964).

TABLE I. $U^{234}(n, f)$ fission-fragment angular distributions.

E_n (keV)	Mean angle θ							
	4.8°	12.5°	17.5°	22.5°	27.5°	32.5°	38.2°	42.5°
200	590±80	644±75	672±63	668±56	629±50	550±44	536±65	492±51
300	349±62	364±60	359±45	388±43	391±39	389±34	407±60	426±51
400	1000±104	1160±106	1344±87	1487±83	1575±78	1639±69	1872±125	1831±102
500	2237±167	2487±159	2843±139	3234±136	3219±125	3542±122	3710±189	4063±191
600	3119±185	3574±208	3817±178	3989±162	3951±147	4042±130	4062±185	3948±150
700	5977±254	6260±274	6424±224	6553±204	6649±187	6803±194	7115±243	7344±204
843	9794±326	10004±339	9697±276	9511±244	8825±214	8465±181	8315±275	7418±214
998	3959±389	3739±386	4187±308	4292±288	4064±256	3878±215	3780±304	3600±244
1184	2073±297	2605±310	2723±260	2673±229	2576±204	2212±164	2736±276	2424±214
E_n (keV)	47.5°	52.5°	59.0°	67.0°	72.5°	77.5°	82.5°	87.5°
200	440±45	421±44	443±34	439±38	424±42	420±40	401±40	387±56
300	443±49	406±46	411±34	362±37	350±41	364±40	347±40	321±39
400	1770±93	1819±95	1843±69	1759±75	1633±82	1564±77	1603±110	1558±111
500	4204±162	4346±165	4496±141	4430±130	4711±151	4348±142	4196±143	4105±156
600	3905±138	3847±140	4025±110	3740±130	3595±136	3507±130	3494±132	3436±134
700	7277±193	7538±192	7364±140	7245±210	6808±229	6617±216	6243±223	5724±208
843	7017±197	6715±191	6245±172	5899±167	5618±178	5696±171	5680±211	5501±208
998	3751±231	3747±232	4121±179	3924±197	3804±220	3881±212	3626±207	3561±226
1184	2218±189	2110±186	2258±139	2169±146	2001±159	2195±158	2026±156	1795±148

The detector was 200 μ thick. It was arranged in the form of a truncated cone at the base, supporting a cylindrical section, which in turn supported a top cone. The top cone was sliced at an angle of 33° so that an elliptical section is at the top near the polar angle of 0°. The reasons for choosing this geometry are: (a) it guarantees that all fission fragments from a source at the center of the base of the bottom cone will enter the detector material at angles between 20° and 70°, thus ensuring proper track registration; (b) the symmetry of the detector ensures rapid reading of the data since all the tracks along a circular ring perpendicular to the axis of symmetry (the beam axis) will correspond to the same angle θ ; and (c) it affords the 2π geometry necessary for measuring angular distributions in the low cross-section region near threshold. Both the U^{234} target and the detector were enclosed in a thin-walled, evacuated aluminum scattering chamber. After irradiation, the detector material was chemically etched (6*N* NaOH for 40 min at 70°C for 50 h at room temperature), and the resulting fragment "tracks" were viewed with an optical microscope.

In order to read the data one merely counts the number of fragment tracks for a given circular ring perpendicular to the symmetry axis (the beam direction) on a conical or cylindrical portion of the detector. The corresponding angle θ which the fragment made with the beam direction is calculated from distance measurements on the known geometrical configuration. For the cylinder, an ordinary microscope stage with x - y motion can be used to count the number of fission tracks for grouping them into $\Delta\theta$ intervals. In order to count the tracks on the cones, a mechanically rotating microscope stage was designed and built. The stage rotates the detector so that all the tracks corresponding to a constant angle θ will sweep past the field of view.

The center of curvature can be moved along the y axis so that adjacent strips can be scanned. A dial gauge is attached to the y motion for precision placement of the center of curvature of the arcs to be scanned.

In order to check the accuracy of this method of measuring fission-fragment angular distributions, the fragment angular distribution from the spontaneous fission of Cf^{252} was measured. The measured distribution was isotropic, as expected, within the experimental uncertainties ($\pm 10\%$).

III. EXPERIMENTAL RESULTS

The fission-fragment angular distributions for the $U^{234}(n, f)$ reaction have been measured for average incident neutron energies of 200, 300, 400, 500, 600, 700, 843, 998, and 1184 keV. The raw data were corrected for the experimental angular resolution of 9° due to (a) the size of the proton beam spot on the Li^7 target, (b) the size of the U^{234} target, and (c) the summing over finite scanning area. The data were not corrected for fission induced by neutrons scattered from the chamber walls and components because the calculated magnitude of the effect was small (between 2 and 5% for all neutron energies).⁴ The number of fissions produced by neutrons from the $Li^7(p, n)Be^{7*}$ reaction which leaves Be^7 in its first excited state was negligible at neutron energies $E_n \leq 843$ keV. At the two highest energies, $E_n = 998$ keV and $E_n = 1184$ keV, a correction (of a few percent) was made for the fission events induced by the lower-energy neutron group. (The low-energy neutron groups for $E_n = 998$ keV and $E_n = 1184$ keV are 500 and 700 keV, respectively.)

The corrected experimental results are shown in Fig. 3 and Table I. Note that at 200 and 843 keV, the

⁴ A. N. Behkami, Ph.D. thesis, Northwestern University, 1967 (unpublished).

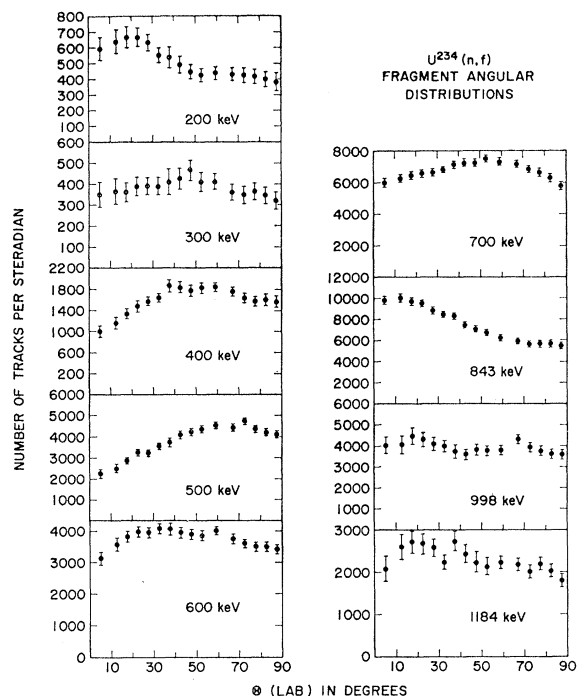


FIG. 3. Fission-fragment angular distributions for the $U^{234}(n,f)$ reaction at several incident neutron energies. The data have been corrected for the experimental angular resolution and in the case of the 998- and 1184-keV data, the data have been corrected for fission events induced by the low-energy neutrons from the $Li^7(p,n)Be^{7*}$ reaction which leaves Be^7 in its first excited state.

angular distributions show prominent peaks near 0° but that at the intermediate energies, the angular distributions peak at angles between 0° and 90° . The anisotropy values $\sigma_f(0^\circ)/\sigma_f(90^\circ)$ are plotted in Fig. 4 as a function of the incident neutron energy. Also shown is the experimental data of Lamphere.⁵ As one can see, the two measurements agree within their experimental uncertainties.

IV. THEORY

The initial step in the (n,f) reaction may be said to be the formation of a compound nucleus. This compound nucleus may decay by (a) the emission of γ rays, (b) the emission of neutrons, or (c) fission. In (a) states of the compound nucleus are populated, in (b) states of the target nucleus are populated, and in (c) states of the transition nucleus are populated. By doing a type of Hauser-Feshbach⁶ calculation, the partial cross sections for fission involving states of the transition nucleus of given (K,π) can be calculated. Combining these partial cross sections with the $W_{MK^J}(\theta)$ functions (see Sec. I) allows one to calculate the total fission cross section σ_f and the differential fission cross section $d\sigma_f/d\Omega(\theta)$. If one is allowed to characterize the probability of

fission involving given states of the transition nucleus by a simple expression using only a few free parameters, then one may reverse the calculation described above and, by sophisticated curve fitting, deduce the K , π , energy and barrier shape of each transition-state fission channel in U^{235*} from our measured angular distributions and the cross-section measurements of Lamphere.⁵ The details of this procedure are given below.

A. Basic Formalism

For the neutron bombardment of an even-even nucleus, the Breit-Wigner formula for the cross section for partial-wave l , entrance channel α , and exit channel α' near an isolated resonance λ of total angular momentum J gives

$$\sigma_{Jl}^{\alpha\alpha'} = \frac{1}{2}(2J+1) \left(\frac{\pi}{k^2}\right) \frac{\Gamma_{\lambda J l}^{(\alpha)} \Gamma_{\lambda J l}^{(\alpha')}}{(E_\lambda - E)^2 + (\Gamma_{\lambda J}/2)^2}, \quad (3)$$

where E_λ is the resonance energy, $k/2\pi$ is the wave number of the incident neutron, $\Gamma_{\lambda J l}^{(\alpha)}$ is the partial width for entrance channel α , $\Gamma_{\lambda J l}^{(\alpha')}$ is the partial width for exit channel α' , and $\Gamma_{\lambda J}$ is the total width of the resonance. Experimentally measured cross sections average over many such resonances. This gives

$$\langle \sigma_{Jl}^{\alpha\alpha'} \rangle = (2J+1) \left(\frac{\pi^2}{k^2}\right) \frac{1}{\langle D_{\lambda J} \rangle} \left\langle \frac{\Gamma_{\lambda J l}^{(\alpha)} \Gamma_{\lambda J l}^{(\alpha')}}{\Gamma_{\lambda J}} \right\rangle \quad (4)$$

for the average cross section where $\langle D_{\lambda J} \rangle$ is the average spacing between resonances of a given total angular momentum and parity. Since the average of a ratio is

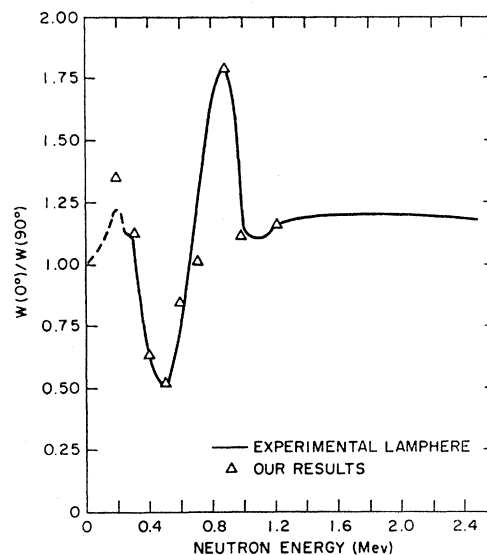


FIG. 4. The fission-fragment anisotropies $\sigma(0^\circ)/\sigma(90^\circ)$ as a function of the incident neutron energy for the $U^{234}(n,f)$ reaction. The triangles indicate our experimental data, and the solid line represents the data of Lamphere (Ref. 5).

⁵ R. W. Lamphere, in *Physics and Chemistry of Fission* (International Atomic Energy Agency, Vienna, 1965), Vol. I, p. 63.

⁶ W. Hauser and H. Feshbach, *Phys. Rev.* **87**, 366 (1952).

not, in general, equal to the ratio of the averages, one cannot substitute

$$\frac{\langle \Gamma_{\lambda J l}^{(\alpha)} \rangle \langle \Gamma_{\lambda J l}^{(\alpha')} \rangle}{\langle \Gamma_{\lambda J} \rangle} \text{ for } \left\langle \frac{\Gamma_{\lambda J l}^{(\alpha)} \Gamma_{\lambda J l}^{(\alpha')}}{\Gamma_{\lambda J}} \right\rangle,$$

so one defines a quantity $S_{\alpha\alpha'}$ (the level-width fluctuation correction factor) as

$$S_{\alpha\alpha'} = \frac{\langle \Gamma_{\lambda J l}^{(\alpha)} \Gamma_{\lambda J l}^{(\alpha')} / \Gamma_{\lambda J} \rangle}{\langle \Gamma_{\lambda J l}^{(\alpha)} \rangle \langle \Gamma_{\lambda J l}^{(\alpha')} \rangle / \langle \Gamma_{\lambda J} \rangle} \quad (5)$$

and obtains

$$\langle \sigma_{J l}^{\alpha\alpha'} \rangle = \frac{\pi^2}{k^2} (2J+1) \frac{\langle \Gamma_{\lambda J l}^{(\alpha)} \rangle \langle \Gamma_{\lambda J l}^{(\alpha')} \rangle}{\langle D_{\lambda J} \rangle \langle \Gamma_{\lambda J} \rangle} \times S_{\alpha\alpha'}. \quad (6)$$

Use of Eq. (6) along with the appropriate summations allows one to calculate the various partial fission, neutron, and γ -ray emission cross sections.

B. Detailed Assumptions Involved in the Calculation

The level-width fluctuation correction factor $S_{\alpha\alpha'}$ is calculated by (a) assuming that the partial widths for different entrance and exit channels are not correlated, and (b) assuming that the partial widths are distributed according to a χ^2 family of distributions, i.e.,

$$P_\nu(X) dX = \frac{1}{2} \nu [\text{gamma function } \frac{1}{2} \nu]^{-1} \times \left(\frac{1}{2} \nu X \right)^{\frac{1}{2}(\nu-2)} e^{-\frac{1}{2} \nu X} dX, \quad (7)$$

where ν is the number of degrees of freedom of the distribution and $X = \Gamma / \langle \Gamma \rangle$. If the partial widths are assumed to have a χ^2 distribution with one degree of freedom (a Porter-Thomas distribution), then $S_{\alpha\alpha'}$ varies from 1 to $\frac{1}{2}$ for $\alpha \neq \alpha'$ and from 1 to 3 for $\alpha = \alpha'$, i.e., an enhancement of compound elastic scattering. The relative magnitude of $S_{\alpha\alpha'}$ decreases for an increasing number of exit channels.

We replaced the neutron entrance- and exit-channel partial widths in Eq. (4) with optical-model transmission coefficients using the relation

$$T_{\lambda J l} = (2\pi / \langle D_{\lambda J} \rangle) \langle \Gamma_{\lambda J l}^{(\alpha)} \rangle. \quad (8)$$

In our calculation, we have assumed that direct interactions are negligible so that proper compound-nucleus transmission coefficients can be approximated as being equal to the optical-model transmission coefficients. The calculations were done using transmission coefficients derived from the Perey-Buck optical-model potential. (The effect of the different optical-model potentials upon the calculations is discussed in Sec. VI.) The widths for each neutron partial wave were assumed to be distributed according to a Porter-Thomas⁷ distribution. The available levels of the residual nucleus U²³⁴ are given in Table II.⁸

The partial widths for γ -ray decay of the compound nuclear state λ with total angular momentum J , parity π , and excitation energy U in Eq. (6) were replaced by

TABLE II. Low-lying levels in U²³⁴.^a

Energy (keV)	Total angular momentum	Parity
0.000	0	+
0.044	2	+
0.143	4	+
0.296	6	+
0.499	8	+
0.790	1	-
0.811	0	+

^a Taken from Ref. 8.

transmission coefficients using the expression⁹

$$T_{\lambda\gamma}(J, \pi, U) = 2\pi \langle \Gamma_{\lambda\gamma}(J, \pi, U) \rangle \rho(J, \pi, U), \quad (9)$$

where $\rho(J, \pi, U)$ is the density of (J, π) levels at excitation energy U . The energy dependence of the average radiation width was given by the Blatt-Weisskopf formula for dipole γ -ray emission

$$\Gamma_{\lambda\gamma}(U) = C_1 \int_0^U \frac{\rho(U-E)}{\rho(U)} E^3 dE, \quad (10)$$

with Ericson's formulation of the energy dependence of the level density⁹

$$\rho(U) = C_2 \exp(2\pi^2 U / 3\delta)^{1/2}. \quad (11)$$

In the above equations, C_1 , C_2 , and δ are constants, the latter being of the order of the average spacing between single-particle levels. Thus the energy dependence of $T_{\lambda\gamma}$ was given by the function

$$X(U, \delta) = e^x [x^4 - 10x^3 + 45x^2 - 105x + 105],$$

where $x \equiv (2\pi^2 U / 3\delta)^{1/2}$. The functional form of the angular momentum dependence of the level density was given by

$$F(J) = \exp(-J^2 / 2\sigma^2) - \exp(-(J+1)^2 / 2\sigma^2), \quad (12)$$

where σ is the familiar spin-cutoff parameter. Combining Eqs. (9)–(12), we get

$$T_{\lambda\gamma}(J, \pi, E) = 2\pi \left(\frac{\Gamma_\gamma}{D} \right)_0 \frac{F(J, \sigma) X(U_0 + E, \delta)}{[F(\frac{1}{2}, \sigma)] X(U_0, \delta)}, \quad (13)$$

where $(\Gamma_\gamma / D)_0$ is the measured ratio of the average radiation width to level spacing for compound nuclear states populated by s -wave neutrons of zero energy, E is the neutron energy, and U_0 is the neutron binding energy. In the actual calculations, the numerical values used were $(\Gamma_\gamma / D)_0 = 0.0016$, $\sigma = 6$, $\delta = 0.200$ MeV, and $U_0 = 5.27$ MeV.

The partial widths for fission through an exit channel

⁷ C. E. Porter and R. G. Thomas, Phys. Rev. 104, 483 (1956).

⁸ E. K. Hyde, I. Perlman, and G. T. Seaborg, *The Nuclear Properties of the Heavy Elements* (Prentice-Hall, Inc., Englewood Cliffs, N. J., 1964), Vol. II, p. 659.

⁹ P. A. Moldauer, C. A. Engelbrecht, and G. J. Duffy, Argonne National Laboratory Report No. ANL-6978, 1964 (unpublished).

TABLE III. Low-lying low angular momentum states of the U^{235} transition nucleus.

(K, π)	E_0 (keV)	$\hbar\omega$ (keV)
$\frac{1}{2}^+$	600	625
$\frac{3}{2}^+$	375	275
$\frac{5}{2}^+$	550	300
$\frac{7}{2}^+$	>500	...

of given (J, K, π) were replaced by transmission coefficients given by

$$T_{\lambda f}(J, K, \pi, E) = (2\pi / \langle D_{\lambda J} \rangle) \langle \Gamma_{\lambda f}(J, \pi, K, E) \rangle. \quad (14)$$

In order to calculate the transmission coefficients for fission, the fission barrier was assumed to have the shape of an inverted parabola. Hill and Wheeler¹⁰ have shown that the penetrability is then given by the expression

$$T_f(J, K, \pi, E) = \{1 + \exp[2\pi(E_f(J, K, \pi) - E_n)/\hbar\omega]\}^{-1}, \quad (15)$$

where E_n is the incident neutron energy, $E_f(J, K, \pi)$ is the fission barrier height (relative to the neutron binding energy) associated with the state (J, K, π) of the transition nucleus, and $\hbar\omega$ is the barrier curvature. This barrier curvature $\hbar\omega$ is inversely proportional to the thickness of the fission barrier. Thus, for small values of $\hbar\omega$, one has a thick barrier and one gets little barrier penetration until one is very near the top of the barrier. The barrier height $E_f(J, K, \pi)$ was calculated using the expression

$$E_f(J, K, \pi) = E_0 + (\hbar^2/2\mathcal{J}_1)[J(J+1) - \alpha(-1)^{J+\frac{1}{2}}(J+\frac{1}{2})\delta_{K, \frac{1}{2}}], \quad (16)$$

where E_0 is a constant, \mathcal{J}_1 is the effective moment of inertia about an axis of rotation perpendicular to the nuclear symmetry axis, α is the familiar decoupling constant for $K=\frac{1}{2}$ bands, and $\delta_{K, \frac{1}{2}}$ is the Kronecker δ . The values of (K, π) chosen for each state of the transition nucleus govern the allowed values of J and the allowed values of l , the orbital angular momentum transfer, to reach a given J . In our calculations the fission widths were assumed to be distributed in a Porter-Thomas⁷ distribution.

Having thus defined the various quantities and explained how they were calculated, Eq. (6) was used to calculate the partial fission cross sections for each member (J, π) of the rotational band built upon a particular state of the transition nucleus (K, π) . For a state of particular (J, K, M) the fragment angular distribution $W_{MK}^J(\theta)$ is given by Eq. (4) and hence, the fission-fragment angular distribution associated with fission through a state of given K is readily computed from

$$W_K(\theta) = \sum_{J, \pi, M} \sigma_f(J, K, \pi) W_{MK}^J(\theta) \quad (17)$$

¹⁰ D. L. Hill and J. A. Wheeler, Phys. Rev. 89, 1102 (1953).

once the various partial fission cross sections are known. The actual calculations of the various partial fission cross sections and angular distributions taking into account level-width fluctuations were done using the computer program WILDCAT¹¹ which is an extended version of the NEARREX program of Moldauer *et al.*⁹

Thus, using the formalism described above, we were able to calculate the fission cross section and angular distribution for any incident neutron energy by specifying the number of accessible states of the transition nucleus and the K, π, E_0 , and $\hbar\omega$ associated with each state. In actual practice, of course, the procedure is reversed. One tries to obtain the best fit to the energy variation of the experimental cross section and angular distribution data by juggling (a) the number of accessible states of the transition nucleus and (b) the parameters K, π, E_0 , and $\hbar\omega$ associated with each of these states.

V. RESULTS OF THE CALCULATIONS

We have attempted to fit the energy variation of the total fission cross section and the fragment angular distributions in the energy region from $E_n=200$ keV to $E_n=1184$ keV. Using the theoretical framework

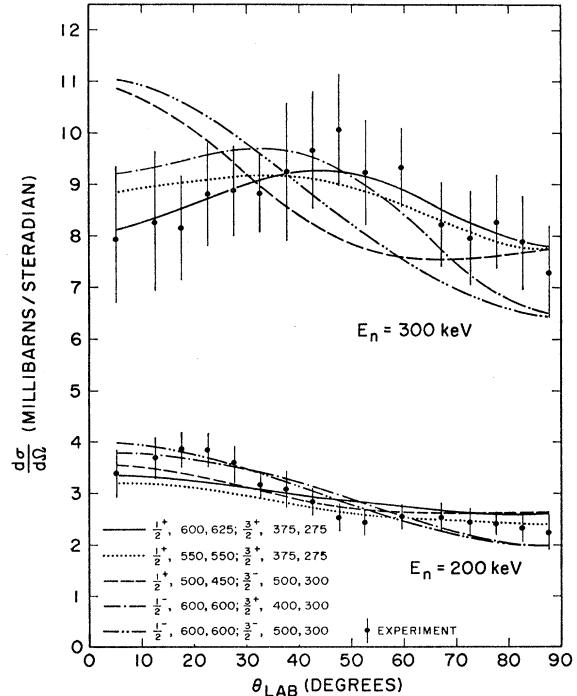


FIG. 5. Fission-fragment angular distributions for the $U^{234}(n, f)$ reaction at $E_n=200$ and 300 keV. The points are the experimental data and the curves represent our "best fits" to the angular distributions and cross sections with *two* accessible states of the transition nucleus. The transition-state parameters for these "best fit" curves are given on the figure. The notation $\frac{1}{2}^+$, 600, 625 means $(K, \pi) = \frac{1}{2}^+$, $E_0=600$ keV, and $\hbar\omega=625$ keV.

¹¹ This program is available, upon request, from the authors.

described in Sec. IV, and after an extensive search of the possible number of accessible states of the transition nucleus and the possible values of the free parameters K , π , E_0 , and $\hbar\omega$ for each state, we have concluded that the experimental data can be adequately described in the energy region from $E_n=200$ keV to $E_n=500$ keV by assuming that there are three accessible states of the transition nucleus and that the values of K , π , E_0 , and $\hbar\omega$ are as given in Table III. In the energy region from $E_n=600$ keV to $E_n=1184$ keV our calculations show that more than one, and probably more than two, additional states of the transition nucleus become accessible. At least one of these states must have $K=\frac{1}{2}$.

A simple qualitative explanation of the results shown in Table III can be seen if one considers the data shown in Fig. 3. The peak near 0° in the 200-keV angular distribution indicates the presence of a $K=\frac{1}{2}$ state. The intermediate-angle peaking in the 300-keV angular distribution indicates the presence of a $K \geq \frac{3}{2}$ state. Detailed calculations (see below) indicate that $K=\frac{5}{2}$ states are not excited strongly enough in the $U^{234}(n,f)$ reaction to account for the measured cross sections. Hence the $K=\frac{3}{2}$ state was chosen to be $(K,\pi)=\frac{3}{2}^- + ((K,\pi)=\frac{3}{2}^- \text{ peaks at } 90^\circ)$. However, the continued strong intermediate-angle peaking at 400 and 500 keV with the shifting of the peak towards 90° and the strong increase in cross section in this energy region indicates the presence of another $K=\frac{3}{2}$ state, this time a

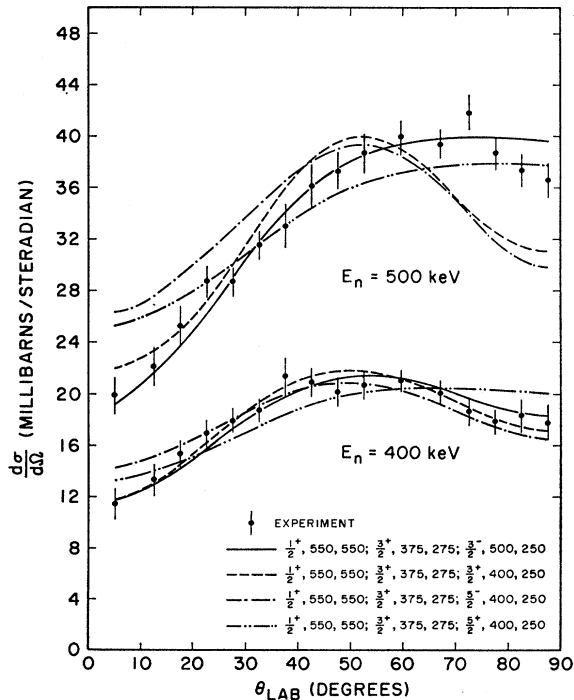


FIG. 6. Fission-fragment angular distributions for the $U^{234}(n,f)$ reaction at $E_n=400$ and 500 keV. The points are the experimental data and the curves represent our "best fits" to the angular distributions and cross sections with three accessible states of the transition nucleus. The notation is the same as Fig. 5.

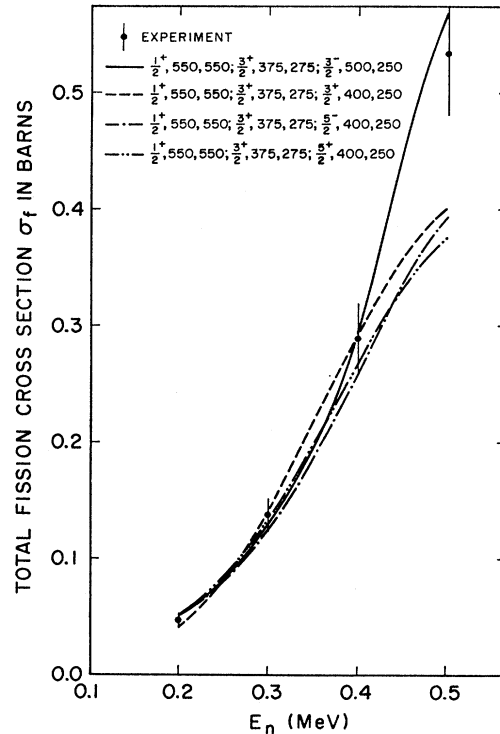


FIG. 7. Total fission cross section for the $U^{234}(n,f)$ reaction as a function of incident neutron energy; $E_n=200, 300, 400,$ and 500 keV. The points are the experimental data of Lamphere (Ref. 5) with a $\pm 10\%$ uncertainty as indicated by the work of Davey (see Ref. 12). The curves show our "best fit" calculations which include level-width fluctuation corrections. The notation is the same as Fig. 5.

$(K\pi)=\frac{3}{2}^-$ ($-$ parity to provide the necessary increase in cross section). Finally, the strong peak at 0° in the 843-keV angular distribution indicates the presence of another $K=\frac{1}{2}$ state.

To guide us in a quantitative evaluation of the agreement between theory and experiment, we used the χ^2 criterion to reject unsatisfactory hypotheses. Each hypothesis tested consisted of two parts, the calculational framework described in Sec. IV and a particular choice of the free parameters K , E_0 , $\hbar\omega$, and π . Unsatisfactory hypotheses were rejected at the 0.05 level of significance. Although we reached reasonable choices of K , E_0 , $\hbar\omega$, and π we made only a limited search of different forms of the calculational framework. Therefore, we are saying that *using the theoretical approximations described in Secs. IV and VI as a basis for calculation*, we can reject all unsatisfactory values of the free parameters with only one chance in twenty of being in error.

In making our search for acceptable hypotheses to describe the data, we have assumed that we should use the minimum number of accessible states of the transition nucleus at any given energy. This assumption, made for simplicity and precision in the determination of the free parameters, means that there may be many

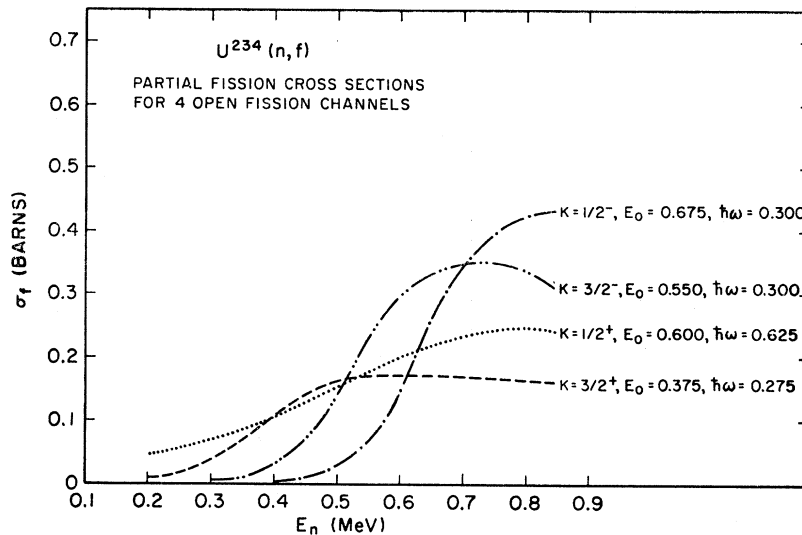


FIG. 8. Summary of the parameters describing the accessible states of the transition nucleus and the partial fission cross section associated with each state as a function of the incident neutron energy. The energies are given in MeV. A possible fourth state in the transition nucleus is also shown.

hypotheses involving weakly excited states which will fit the data. We simply cannot say anything about them.

Beginning with the case of the data from two neutron energies, $E_n=200$ and 300 keV, and two accessible states of the transition nucleus, we found, after extensive searching, that we could reject all hypotheses not assigning values of $\frac{1}{2}+$ and $\frac{3}{2}+$ for the K, π of these two states. A few sample fits to the angular distributions are shown in Fig. 5. We found that the data at 400 and 500 keV could be adequately described by adding a third accessible state in the transition nucleus and assigning values of $(K, \pi) = \frac{3}{2}-$. The fits to the 400 - and 500 -keV angular distributions and the total fission cross section¹² are shown in Figs. 6 and 7.

Detailed calculations revealed that the values of E_0 and $\hbar\omega$ given in Table III should be regarded as uncertain to at least ± 50 – 100 keV. The partial fission cross sections are shown in Fig. 8.

Further attempts to fit the data from $E_n=200$ keV to $E_n=843$ keV by adding a fourth and fifth accessible state in the transition nucleus were unsuccessful. The best attempts at fitting this data are shown in Figs. 9 and 10, although it should be understood that these are not satisfactory fits to the data when judged by a χ^2 criterion. About all that can be said is that there must be at least one more accessible state of the transition nucleus with $K=\frac{1}{2}$ coming into play before $E_n=843$ keV.

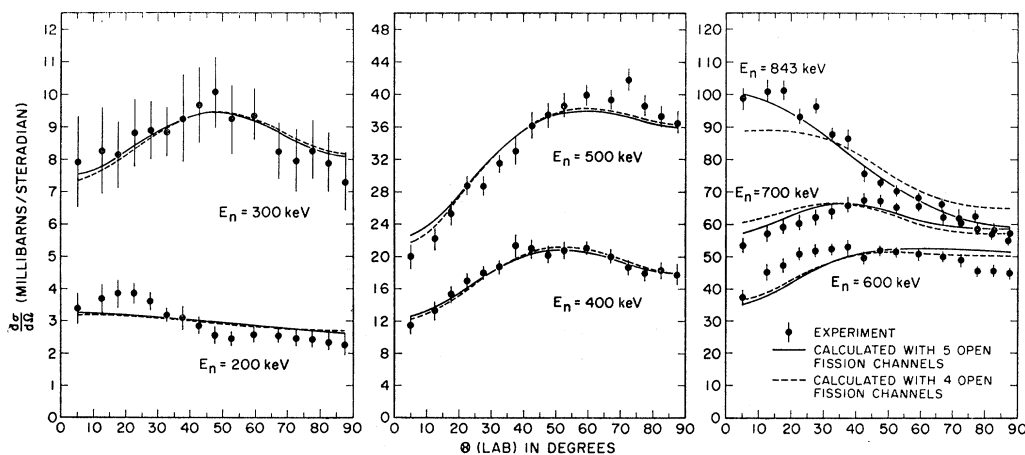


FIG. 9. Fission-fragment angular distributions for the $U^{234}(n, f)$ reaction at seven incident neutron energies. The points are the experimental data and curves represent our "best fits" with *four* and *five* accessible states of the transition nucleus. The parameters for these best fits are as follows: four states— $\frac{1}{2}+$, $600, 625$; $\frac{3}{2}+$, $375, 275$; $\frac{3}{2}-$, $550, 500$; and $\frac{1}{2}-$, $675, 300$; five states— $\frac{1}{2}+$, $600, 625$; $\frac{3}{2}+$, $375, 275$; $\frac{3}{2}-$, $550, 300$; $\frac{1}{2}-$, $750, 150$; and $\frac{1}{2}-$, $725, 400$. E_0 and $\hbar\omega$ for each state are given in keV.

¹² W. G. Davey, Nucl. Sci. Engr. 26, 149 (1966).

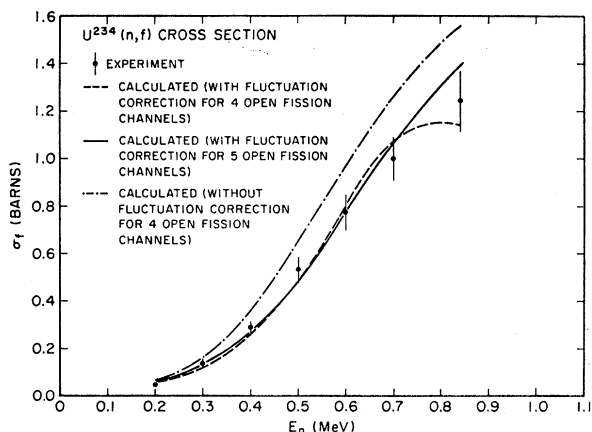


FIG. 10. Total fission cross section for the $U^{234}(n,f)$ reaction as a function of incident neutron energy. The points represent the experimental data of Lamphere (Ref. 5). The curves show the "best fit" calculations for the case of *four* and *five* open fission channels (including level-width fluctuation corrections). The dot-dash curve was computed with the same parameters as the dashed curve (four open fission channels with fluctuation correction) except that the level-width fluctuation corrections were not included. The parameters of the states are given in the caption of Fig. 9.

VI. UNCERTAINTIES IN THIS METHOD OF TRANSITION STATE SPECTROSCOPY

In Sec. V we described the procedure whereby we searched over the set of all possible values of K , E_0 , $\hbar\omega$, and π as well as the number of accessible states of the transition nucleus to find a set of parameters which described the data adequately. In order to further test the meaningfulness of these results, we changed much of the input data for the calculations, redid the search to find new values of K , E_0 , π , and $\hbar\omega$, and compared these new values to those obtained previously. The

TABLE IV. Range of variation of input parameters in calculation.

Input parameter	Description	Range of variation	Significant effect on χ^2 ?
$\hbar^2/2\mathcal{I}_1$	rotational constant	2.5-7.5 keV	No
α	decoupling constant	-3-+3	No
ν_f	degrees of freedom of Γ_γ distribution	1, 2	No
$(\Gamma_\gamma/D)_0$	ratio of capture width to level spacing for slow neutron capture	0.0012-0.0022	No
σ	spin-cutoff parameter	4-6	No
δ	single-particle level spacing	0.1-0.2 MeV	No
U	neutron binding energy	5-8 MeV	No

input parameters varied and the results of these calculations are shown in Table IV.

As one can see from examining Table IV, the range in values of the input parameters describing the γ -ray decay channels and the fission decay channels which still give significant fits to the data (when judged by a χ^2 criterion) spans the range of physically reasonable values of these parameters. In addition, we have repeated the determination of K , E_0 , $\hbar\omega$, and π using the Bjorklund-Fernbach optical-model transmission coefficients instead of the Perey-Buck coefficients¹³ used to get the results discussed in Sec. V. As one can see by examining Figs. 11 and 12, there is no significant difference in the quality of the fits obtained with either set of transmission coefficients. Furthermore, a detailed search showed that one would arrive at exactly the same conclusions as to the values of E_0 , K , π , and $\hbar\omega$ regardless of the optical-model potential chosen. As one can see from examining Fig. 10, the inclusion of level-width fluctuation corrections significantly lowers the calculated fission cross section. Such a loss in cross

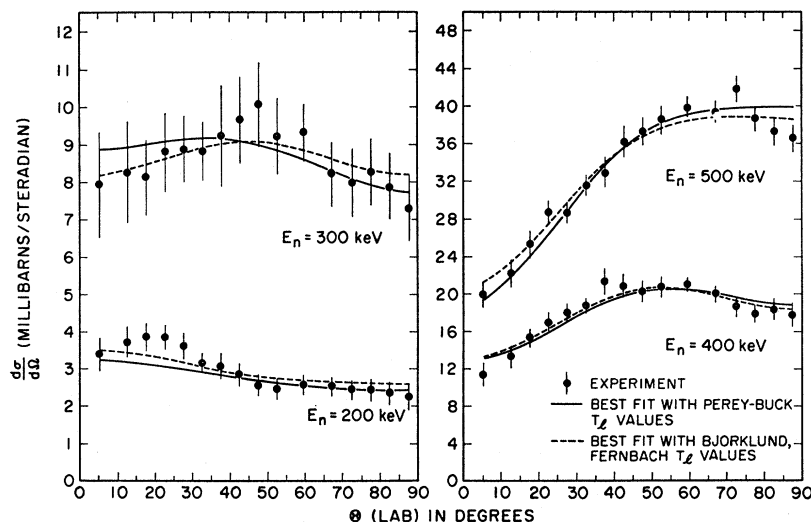


FIG. 11. Fission-fragment angular distributions for the $U^{234}(n,f)$ reaction at incident neutron energies of $E_n=200, 300, 400,$ and 500 keV. The points are the experimental data and the curves represent the "best fit" for *three* open fission channels and two choices of neutron transmission coefficients, namely, those of Perey-Buck (Ref. 13) and Bjorklund-Fernbach (Ref. 13). The transition-state parameters for the Perey-Buck fit are the same as those of the solid line in Fig. 6.

¹³ Both the Bjorklund-Fernbach and Perey-Buck optical-model transmission coefficients were obtained from E. Auerbach and F. Perey, Brookhaven National Laboratory Report No. BNL-765 (T-286), 1962 (unpublished).

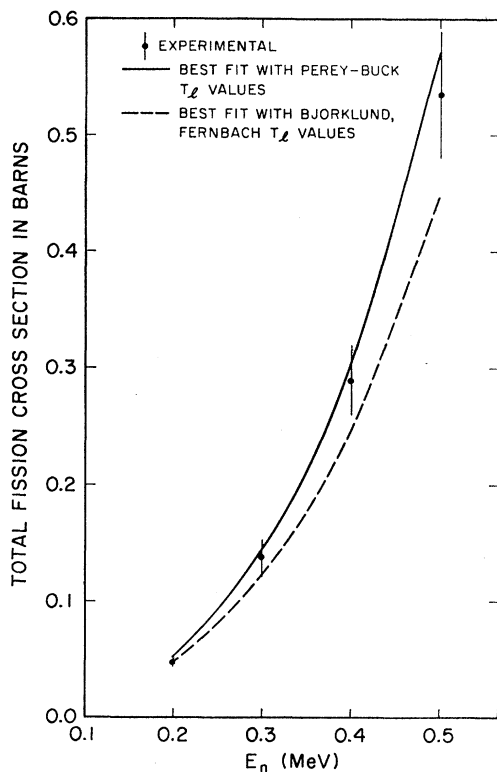


FIG. 12. Total fission cross section for the $U^{234}(n,f)$ reaction as a function of the incident neutron energy from $E_n=200$ keV to $E_n=500$ keV. The points represent the experimental data of Lamphere (Ref. 5). The curves represent the "best fit" calculations for three open fission channels and two choices of neutron transmission coefficients, namely, those of Perey-Buck (Ref. 13) and Bjorklund-Fernbach (Ref. 13). The parameters are the same as those in Fig. 11.

section can be regained by juggling the E_0 and $\hbar\omega$, but their values would probably have to be changed far more than the 50–100 keV uncertainty now associated with these parameters.

VII. COMPARISON OF RESULTS WITH OTHER DATA, CALCULATIONS, ETC.

Lamphere, in a previous analysis⁵ of the fission-fragment anisotropies for the $U^{234}(n,f)$ reaction, concluded that states with $(K,\pi)=\frac{1}{2}+, \frac{3}{2}-$, and $\frac{1}{2}-$ had to be present. Our analysis, with complete fragment angular distributions available to us, also indicates the presence of these three states as well as a $(K,\pi)=\frac{3}{2}+$ state. We believe that our analysis, because of its detailed consideration of the competition between the various modes of decay of the compound nucleus and the simultaneous fitting of both the fission cross section and angular distributions, is superior to that of Lamphere.

Vandenbosch, in a recent analysis¹⁴ of the energy variation of the fission cross section and fragment anisotropies, concluded that "no firm, unique K -band

assignments for neutron-induced fission of thorium, uranium, or plutonium can be made." Speaking in an absolute sense, this statement is completely correct. However, within the framework of our simple, approximate model of fission-barrier penetration (which closely resembles the one used by Vandenbosch) we can uniquely and firmly make assignments of the (K,π) of the states of the transition nucleus U^{235*} . It is true that we make some simplifying and probably wrong assumptions in our calculations (i.e., smooth rather than "lumpy" fission barriers, same value of $\hbar\omega$ for each member of a rotational band), but the fact remains that we are able to reproduce the values of the fission cross section and angular distributions for the low-energy neutron-induced fission of U^{234} using this model. Perhaps the ultimate meaningfulness of this calculational procedure and the (K,π) assignments derived from it depends on just how much of the data on neutron-induced fission can be understood using these concepts. Further work concerning this point is now in progress.

Detailed comparison of the (K,π) assignments made in this work with nuclear-structure calculations based on extensions of the Nilsson model to high deformations do not seem to be meaningful at this point because of the great uncertainty as to what the Nilsson model predicts for deformations corresponding to the transition-state nucleus.¹⁵ However, one does note in examining such calculations that states of $K \geq \frac{5}{2}$ do occur quite frequently near the fission barrier. Some experimental evidence is available from studies of the $U^{234}(d,pf)$ reaction¹⁶ that there are low-lying states of the U^{235*} transition nucleus with $(K,\pi) \geq \frac{5}{2}$, but these states are not excited in the (n,f) reaction.

As Vandenbosch points out,¹⁴ one should not be disturbed by differences in the values of $\hbar\omega$ for the various transition states. In an odd- A nucleus the restrictions of conservation of angular momentum and parity do not permit one to exploit all the level crossings in the Nilsson diagram. The average value of $\hbar\omega$ found for the low-lying low angular momentum states of the U^{235*} transition nucleus is ~ 400 keV. This compares reasonably well with the value of ~ 400 keV determined by Halpern¹⁷ from an analysis of spontaneous fission half-lives and photofission thresholds and the upper limit of 620 keV determined by Nix¹⁸ from liquid-drop calculations.

¹⁵ See, for example, the differing predictions of (a) J. R. Primack, Ph.D. thesis, Princeton University, 1966 (unpublished); Phys. Rev. Letters **17**, 539 (1966). (b) S. G. Nilsson, *International School of Physics "Enrico Fermi," Course XL* (Academic Press Inc., New York, 1967); I. L. Lamm, B. Nilsson, S. G. Nilsson, Z. Szymanski, A. Sobiczewski, and S. Wycech (to be published). (c) V. M. Strutinsky, Nucl. Phys. **A95**, 420 (1967).

¹⁶ W. Loveland and J. P. Unik, Bull. Am. Phys. Soc. **12**, 922 (1967).

¹⁷ I. Halpern, Ann. Rev. Nucl. Sci. **9**, 245 (1959).

¹⁸ J. R. Nix, Ann. Phys. (N. Y.) **41**, 52 (1967).

¹⁴ R. Vandenbosch, Nucl. Phys. **A101**, 460 (1967).

VIII. CONCLUSIONS

What have we learned from this study?

(a) We believe that we have demonstrated a novel way of using Lexan polycarbonate to measure fission-fragment angular distributions in the low cross-section region near threshold and have applied the technique to the $U^{234}(n,f)$ reaction.

(b) We believe that we have shown that a proper analysis of the energy variation of the cross section and angular distributions for neutron-induced fission can yield a reasonable quantum-mechanical description of an extremely deformed nucleus, the transition nucleus. We have proposed a simple calculational framework for such analyses and explored some of its uncertainties.

(c) We have shown that the transition-state spectrum of U^{235*} is more complex than had been suggested previously. Furthermore, the intriguing possibility is suggested that the barrier curvature $\hbar\omega$ may differ for different states of the transition nucleus.

ACKNOWLEDGMENTS

We thank Professor Robert Vandenbosch for showing us his results prior to publication and for many helpful discussions of this problem. We also acknowledge valuable discussions with Dr. P. A. Modauer and Dr. A. Jaffey, and J. Lerner for preparation of the U^{234} target on the Argonne National Laboratory mass separator. The staffs and operating crews of the 4-MeV and 3-MeV Van de Graaffs of the Argonne Physics and Reactor Physics Divisions, respectively, were extremely helpful during our many bombardments, and we wish to acknowledge their contributions to these experiments. Some of the calculations which helped to clarify this problem were carried out at Oregon State University with support from an NSF Institutional Grant to the OSU Computer Center. Additional support in the form of a research assistantship was obtained through a NSF Institutional Grant to Northwestern University.

APPENDIX

Before arriving at the detection scheme adopted in this experiment, another method was investigated. This method consisted of placing a thin source of fissionable material in contact with a sheet of polycarbonate resin and deducing the fragment angular distribution from measurements of the directions of the fission tracks in the polycarbonate resin. The track directions were measured with a research microscope equipped with calibrated fine-focus controls and an oil-immersion objective. The projected length, depth difference, and azimuthal angle of each track was measured.

To test the feasibility of this method, collimated beams of fission fragments from the spontaneous fission of Cf^{252} were allowed to enter the resin detector at angles of 20° , 50° , 70° , and 90° with respect to the surface. After irradiation, the detector was etched in 6*N* NaOH at 55°C for 45 min. These etching conditions produced holes of a small diameter that could be clearly seen (except for the 90° exposure) with a $100\times$ oil-immersion objective. By careful observation, it was possible to determine the dip angles of tracks from 20° to 70° with an accuracy of a few degrees. The fission-fragment angular distribution from the spontaneous fission of Cm^{244} was measured using this technique and the expected isotropic angular distribution was observed.

We observed that it was difficult to measure the dip angles of tracks in the angular regions 0° – 20° and 70° – 90° . This difficulty could be surmounted in particle-induced fission studies by having the particle beam strike the fissionable target at an oblique angle and then only accept tracks that make angles of 20° – 70° with the detector surface. The major drawback to this entire experimental technique is the long time required to scan each track. A good scanner can measure only about 30 tracks/h. The scheme is also difficult to automate. The advantage of this technique is that several detector-target assemblies could be irradiated simultaneously.